Nanotechnology

DOI: 10.1002/anie.201402958

Fast Prediction of Adsorption Properties for Platinum Nanocatalysts with Generalized Coordination Numbers**

*Federico Calle-Vallejo, José I. Martínez, Juan M. García-Lastra, Philippe Sautet, and David Loffreda**

Abstract: *Platinum is a prominent catalyst for a multiplicity of reactions because of its high activity and stability. As Pt nanoparticles are normally used to maximize catalyst utilization and to minimize catalyst loading, it is important to rationalize and predict catalytic activity trends in nanoparticles in simple terms, while being able to compare these trends with those of extended surfaces. The trends in the adsorption energies of small oxygen- and hydrogen-containing adsorbates on Pt nanoparticles of various sizes and on extended surfaces were analyzed through DFT calculations by making use of the generalized coordination numbers of the surface sites. This simple and predictive descriptor links the geometric arrangement of a surface to its adsorption properties. It generates linear adsorption-energy trends, captures finite-size effects, and provides more accurate descriptions than d-band centers and usual coordination numbers. Unlike electronic-structure descriptors, which require knowledge of the densities of states, it is calculated manually. Finally, it was shown that an approximate equivalence exists between generalized coordination numbers and d-band centers.*

The increasing global demand for energy, the current dependence on fossil fuels, and the need for carbon-neutral processes call for the use of renewable energy sources and their associated technologies.[1] Among these, catalysis-based technologies, such as fuel cells and electrolyzers, promise to generate, store, and transform clean energy by means of the cleavage and formation of chemical bonds. However, high costs and efficiency and durability problems hinder the widespread implementation of these technologies.[2] The costs are lowered by using nanoparticles, as their high surface area to volume ratio reduces catalyst loadings. The challenge is to find appropriate catalyst sizes and morphologies for given catalytic purposes. Experimentally, this requires facile synthesis methods that permit the preferential formation of active sites with the highest turnover frequencies.[3] From a theoretical standpoint, simple and robust models are required with sound physical–chemical foundations and predictive power, that is, they must be able to univocally locate new information within existing trends. The most successful example of such models is arguably that of Hammer and Nørskov.[4] Their d-band model provides explanations of the reactivity of late transition metals based on a single parameter: the d-band center of the surface atoms. Nevertheless, it requires the computational calculation of projected densities of states (pDOS) on the surface atoms and has some limitations, such as a loss of accuracy for early transition metals, metals with fully filled d-bands, and strongly correlated metals.[5]

Moreover, theoretical chemistry nowadays encounters the need for more realistic descriptions of catalytic nanoparticles. Instead of using model approaches such as Wulff constructions to describe complex nanostructures, first-principles simulations of entire nanoparticles with multiple terrace, edge, and corner sites should be performed to improve the current understanding of catalysis.[6] In this context, the key question is whether it is possible to find simple and efficient descriptors for the reactivity of the multiple sites in nanoparticles and extended surfaces, the variation of which can be unambiguously linked to changes in adsorption energies, and that do not require additional computational calculations to be estimated. In the following we will argue, through the analysis of the adsorption energies of *O, $*O_2$, *OH, *OOH, $*H_2O$, and $*H_2O_2$, that the generalized coordination numbers of surface sites fulfill all those conditions and perform better than conventional descriptors.

The nanoparticles in this study are Pt_{201}, Pt_{79}, and Pt_{38} (Supporting Information, Figure S1). These particles are truncated octahedra with diameters between 0.7 and 1.7 nm, exhibiting hexagonal-type (111) and square-type (100) facets. Besides, there are edges and corners (henceforth referred to as kinks) at the intersection between two and three neighboring terraces, respectively. Adatoms were also added to Pt_{201} in order to increase the types of active sites and explore the properties of highly unsaturated surface Pt atoms (see the Supporting Information). The extended surfaces in this study were carefully chosen to geometrically match the different sites of the nanoparticles, and a full list of crystal facets is given in the Supporting Information (Table S5).

[*] Dr. F. Calle-Vallejo, Dr. P. Sautet, Dr. D. Loffreda
Laboratoire de Chimie, ENS Lyon, Université de Lyon, CNRS
46 Allée d'Italie, 69364 Lyon Cedex 07 (France)
E-mail: david.loffreda@ens-lyon.fr
Dr. J. I. Martínez
Dpto de Superficies y Recubrimientos, ICMM-CSIC
28049 Madrid (Spain)
Prof. J. M. García-Lastra
Dpt of Energy Conversion and Storage, DTU
4000 Roskilde (Denmark)

[**] F.C.V., P.S., and D.L. acknowledge EU funding through the PUMA MIND contract (Call FCH-JU-2011-1, Code SP1-JTI-FCH-2011.1.3, Project 303419). We thank IDRIS and CINES (project 609, GENCI/CT8) and PSMN for CPU time and assistance. J.I.M. acknowledges support from CSIC and ESF through the JAEDoc program. J.M.G.L. acknowledges support from MINECO (FIS2012-30996) and the ReLiable project funded by the DCSR (11-116792).

Supporting information for this article is available on the WWW under http://dx.doi.org/10.1002/anie.201402958.

Coordination numbers are used in chemistry as a zeroth-order approximation to describe the electronic environment in which an atom is embedded. For an fcc crystal, the maximum coordination is obtained in the bulk, where twelve nearest neighbors surround every atom. Coordination numbers below twelve are typical of surfaces and correspond to atoms with tendencies towards the formation of bonds that compensate for the lack of coordination. Hence, there is a proportionality relationship between the lack of coordination of surface atoms and their response towards the formation of new bonds,[7] following bond-order conservation theory.[8] To exemplify this proportionality, the adsorption energies of *OH atop were plotted against the two types of coordination numbers for a multiplicity of adsorption sites on Pt_{38}, Pt_{79}, Pt_{201}, and extended surfaces (Figure 1; for details on the active sites, see Figure S6).

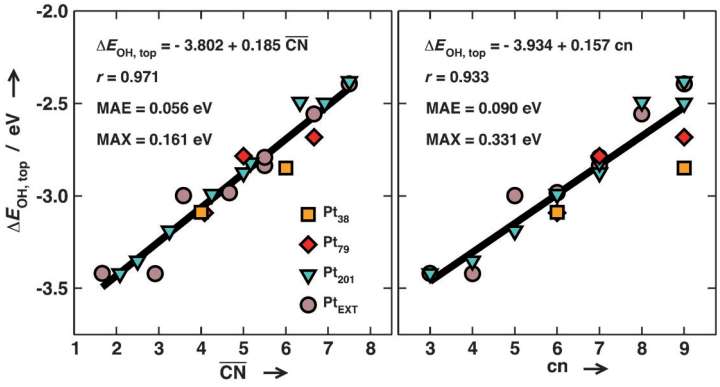

Figure 1. Adsorption energies of *OH atop, described by generalized (left) and usual (right) coordination numbers of the sites to which the adsorbate is bound. Data for Pt_{38} (■), Pt_{79} (◆), Pt_{201} (▼), and extended surfaces (●) are provided. Linear fits and related statistics are also given.

The trends in Figure 1 are described by usual coordination numbers (cn) and a first-order extension of those, which we will refer to as generalized coordination numbers ($\overline{CN}$). To estimate the generalized coordination number ($\overline{CN}$) of an atom i with n_i nearest neighbors, those neighbors are counted and weighted by their own usual coordination numbers [Eq. (1)]:

$$\overline{CN}(i) = \sum_{j=1}^{n_i} \mathrm{cn}(j) n_j / \mathrm{cn}_{\max} \qquad (1)$$

Hence, each neighbor of atom i is not accounted for with a weight of 1, as done usually, but with a weight of $n_j/\mathrm{cn}_{\max}$ (and $\mathrm{cn}_{\max} = 12$ for an fcc crystal). For a top site on a (111) surface, the generalized coordination number of the surface metal atom is thus $\overline{CN} = (9 \times 6 + 12 \times 3)/12 = 7.50$ (as there are six and three neighbors in the first and second layers, respectively, with usual coordination numbers of nine and twelve). The same definition can be extended to bridge sites, where $\mathrm{cn}_{\max} = 18$ (the number of atoms that two nearest-neighbor atoms have in the bulk of an fcc crystal), and to hollow sites, where $\mathrm{cn}_{\max}$ is 22 and 26 for threefold and fourfold sites, respectively (see additional details in Tables S2–S8). We emphasize that double counting of nearest neighbors is avoided, and that generalized coordination numbers 1) can be straightforwardly extended beyond second neighbors, 2) are always smaller than the usual ones (except for the bulk), 3) are bound between 0 and 12 for fcc crystals, as the usual ones, 4) can be used on other lattices, such as bcc crystals, by changing $\mathrm{cn}_{\max}$ accordingly, 5) can be defined on bridge and hollow sites, so that adsorption-mode sensitivity is ensured (see Tables S1–S8 and Figure 2), 6) help distinguish between similar sites in extended surfaces and nanoparticles of various sizes, thereby allowing to quantify size effects.

Figure 1 shows that $\overline{CN}$ performs better than cn, which is mainly due to the limited description of the adsorption-energy trends for small nanoparticles offered by the latter. For instance, the adsorption energies of (111) terraces and kinks on particles of different sizes are clearly distinguished by using $\overline{CN}$ (see Figure S6; see also Figure S3 for a detailed comparison of $\overline{CN}$ and cn). $\overline{CN}$ produces linear relations when plotted against adsorption energies, which suggests that a decrease in coordination number corresponds to an increase in binding strength, as intuitively expected. However, one may argue that the description provided by electronic descriptors, such as d-band centers (ε_d), would be relatively similar, thus questioning whether our new descriptor is advantageous. For comparison, we have plotted the adsorption energies of all oxygen- and hydrogen-containing species against $\overline{CN}$ and ε_d in Figure 2, for the most stable adsorption sites on Pt_{201} and extended surfaces (therefore, top, bridge, and

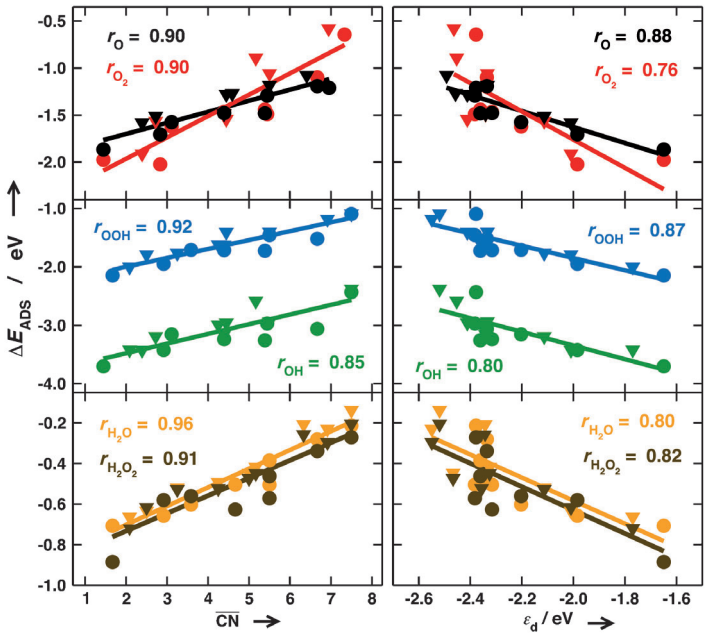

Figure 2. Trends in the adsorption energies of oxygen- and hydrogen-containing species on Pt_{201} (▼) and extended surfaces (●) as a function of $\overline{CN}$ (left) and ε_d (right). Least-square lines and regression coefficients (r) are given in each case (for the corresponding equations, see Table S9).

hollow sites at terraces, edges, and kinks are included). Although ε_d produces similar trends, it is worth noticing (Figure 2) that approximately six to ten sites (depending on the adsorbate) with significantly different adsorption energies have band centers at around -2.34 ± 0.06 eV (see Tables S1 and S5 for the actual values and Figure S2, where the d-band centers were calculated with two different codes). For that narrow distribution of band centers, the ranges of adsorption energies are approximately 0.75 eV for $*O_2$, *OH, and *OOH, and 0.3 eV for *O, $*H_2O$, and $*H_2O_2$. Generalized coordination numbers separate these sites much better and, as a result, yield higher regression coefficients (r; Figure 2; they also yield lower statistical errors, see Table S10), the average of which is 0.91 for $\overline{CN}$ and 0.82 for ε_d.

These features limit the descriptive and predictive power of d-band-based descriptors and furthermore make it difficult to distinguish between important active sites on nanoparticles and extended surfaces. This suggests that the first-moment approximation of the pDOS, which is the cornerstone of the d-band model, is able to capture general trends, but it is not sufficient to differentiate among key sites at the nanoscale. Conversely, $\overline{CN}$ generates rather uniformly distributed trends.

Remarkably, generalized coordination numbers are also able to distinguish between hcp ($\overline{CN}$ =7.50) and fcc ($\overline{CN}$ =6.95) hollow sites in (111) terraces. Such a distinction is not achieved by d-band centers or usual coordination numbers and explains the preference of electronegative adsorbates such as *O for fcc sites. However, the full prediction of preferred adsorption sites, for example, that O prefers the fcc hollow site or OOH the bridge site on Pt(111), requires adsorbate-sensitive descriptors.[9]

The analogous description of adsorption energies provided by $\overline{CN}$ and ε_d in Figure 2 suggests that an explicit physical–chemical relation must exist between geometric and electronic structures. The bond-cutting model provides the simplest relationship between surface energy and usual coordination numbers.[10] As generalized coordination numbers are a first-order extension of the usual ones (see Figure S2), it is possible to apply the bond-cutting model in a similar fashion. Following Eichler et al.[10] (see Section S4), the formation of a surface is a perturbation to the bulk that can be quantified in terms of $\overline{CN}$. The slab formation energy (σ) with respect to the bulk is described by Equation (2):

$$\sigma = E_{stab} - E_{bulk} \approx \frac{E_{COH}}{2}\left(\frac{\overline{CN}_{surf}}{\overline{CN}_{bulk}} - 1\right) \quad (2)$$

Where E_{COH} is the cohesive energy of the material. For simplicity, the correlation between σ and $\overline{CN}$ is assumed to be linear in the coordination range of interest, but approaches exist that correlate those variables as $\sigma = F\left(\overline{CN}^{1/2}\right)$ in wider ranges of coordination[10,11] (see Section S4 for further discussion). On the other hand, following the d-band model,[4] σ can also be approximated as the difference between the average band energies of surface and bulk, multiplied by their average occupations [θ_d; Eq. (3)]:

$$\sigma \approx \theta_d f\left(\varepsilon_d^{surf} - \varepsilon_d^{bulk}\right) \quad (3)$$

where ε_d^{bulk} is constant for a given transition metal, and f is a factor that relates d-band centers calculated up to the Fermi level and over the whole d-band, calculated according to the rectangular band approximation[12] (see Figure S4). The combination of Equations (2) and (3) provides an approximate relationship between $\overline{CN}$ and ε_d [Eq. (4)]:

$$\varepsilon_d^{surf} \approx \varepsilon_d^{bulk} + \frac{E_{COH}}{2\theta_d f}\left(\frac{\overline{CN}_{surf}}{\overline{CN}_{bulk}} - 1\right) \quad (4)$$

The implications of Equation (4) are far reaching. It shows that the d-band center of a given surface atom is approximately equal to that of a bulk atom plus a positive correction that accounts for three main factors: the cohesive energy of the material, the geometric environment in which the surface atom is embedded, and the electronic occupation of its d band. It can be inferred that the correction accounts for the narrowing of the d-band that accompanies surface formation.[4] Interestingly, the explicit relationship between geometric and electronic structures in Equation (4) appears in the literature only through qualitative analyses.[7a,13] To show the accuracy of Equation (4), we present the d-band centers of a multiplicity of atop surface sites on extended surfaces and nanoparticle sites of Pt as a function of $\overline{CN}$ in Figure 3.

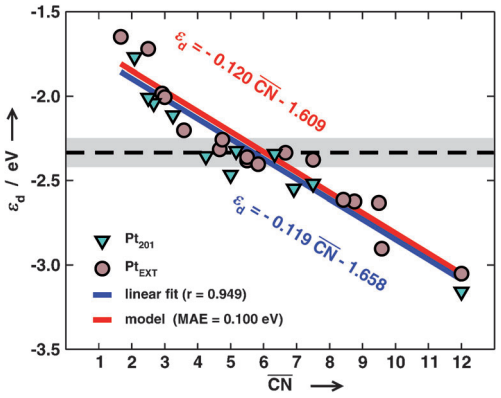

Figure 3. Relationship between $\overline{CN}$ and ε_d for various top sites on Pt_{201} (▼) and extended surfaces (●). The blue line is the least-square fit; the red line corresponds to Eq. (4). The dashed line at −2.34 eV marks the region with nearly identical ε_d, but different $\overline{CN}$ values.

The slopes and offsets of the model and the least-square line are in excellent agreement (0.120 vs. 0.119 and −1.609 eV vs. −1.658 eV), which validates the model. It is also worth mentioning that $\overline{CN}$ is correlated to other electronic-structure descriptors, such as band fillings and half-wave energies (see Figure S5).

Although the overall trend in Figure 3 is practically linear, it is possible to pinpoint the nanoparticle and extended surface sites for which the d-band center has limited accuracy as a descriptor of adsorption energies. The region of points for which ε_d is nearly −2.34 eV corresponds to a range of $\overline{CN}$ from 4 to 7.5. This wide range reaches from poorly coordinated sites, such as kinks and edges, to low-index facets, such as (100) and (111) terraces (see the Supporting Information).

In view of this, d-band centers have limited accuracy for sites that contribute significantly to the overall catalytic properties of Pt, as noted by other authors.[5a,b]

Finally, it is important to note that the accuracy of DFT-GGA energetics can be cautiously set at ± 0.2 eV,[14] which applies to d-band centers and adsorption energies. This means that DFT-predicted catalytic activities can have significant inaccuracies. In contrast, generalized coordination numbers are accurately determined as long as large adsorption-driven reconstructions are not undergone. Thus, $\overline{CN}$ opens the path for improved quantitative predictions of adsorption energies.

To summarize and conclude, we have provided a simple and powerful alternative to electronic-structure analyses for understanding chemical reactivity on pure metals. So far, our descriptor can be applied to metallic nanostructures of various sizes and has not only descriptive, but also predictive power, a solid physical–chemical basis, and does not require the computation of any electronic-structure calculations. The extension to other types of catalysts, such as metal alloys, is the subject of ongoing work.

Experimental Section

The DFT calculations were made with VASP.[15] For full details, see the Supporting Information.

Received: March 4, 2014
Published online: June 11, 2014

Keywords: adsorption energy · coordination numbers · d-band center · nanoparticles · platinum

[1] N. S. Lewis, D. G. Nocera, *Proc. Natl. Acad. Sci. USA* **2006**, *103*, 15729 – 15735.
[2] H. A. Gasteiger, S. S. Kocha, B. Sompalli, F. T. Wagner, *Appl. Catal. B* **2005**, *56*, 9 – 35.
[3] a) F. J. Perez-Alonso, D. N. McCarthy, A. Nierhoff, P. Hernandez-Fernandez, C. Strebel, I. E. L. Stephens, J. H. Nielsen, I. Chorkendorff, *Angew. Chem.* **2012**, *124*, 4719 – 4721; *Angew. Chem. Int. Ed.* **2012**, *51*, 4641 – 4643; b) A. I. Yanson, P. Rodriguez, N. Garcia-Araez, R. V. Mom, F. D. Tichelaar, M. T. M. Koper, *Angew. Chem.* **2011**, *123*, 6470 – 6474; *Angew. Chem. Int. Ed.* **2011**, *50*, 6346 – 6350; c) M. A. Mahmoud, R. Narayanan, M. A. El-Sayed, *Acc. Chem. Res.* **2013**, *46*, 1795 – 1805.
[4] B. Hammer, J. K. Nørskov in *Advances in Catalysis*, *Vol. 45* (Eds.: H. K. Bruce, C. Gates), Academic Press, New York, **2000**, pp. 71 – 129.
[5] a) T. H. Yu, T. Hofmann, Y. Sha, B. V. Merinov, D. J. Myers, C. Heske, W. A. Goddard, *J. Phys. Chem. C* **2013**, *117*, 26598 – 26607; b) T. Hofmann, T. H. Yu, M. Folse, L. Weinhardt, M. Bär, Y. Zhang, B. V. Merinov, D. J. Myers, W. A. Goddard, C. Heske, *J. Phys. Chem. C* **2012**, *116*, 24016 – 24026; c) S. Schnur, A. Groß, *Phys. Rev. B* **2010**, *81*, 033402.
[6] a) V. Viswanathan, F. Y.-F. Wang, *Nanoscale* **2012**, *4*, 5110 – 5117; b) G. A. Tritsaris, J. Greeley, J. Rossmeisl, J. K. Nørskov, *Catal. Lett.* **2011**, *141*, 909 – 913; c) L. Wang, A. Roudgar, M. Eikerling, *J. Phys. Chem. C* **2009**, *113*, 17989 – 17996.
[7] a) A. Groß, *J. Comput. Theor. Nanosci.* **2008**, *5*, 894 – 922; b) A. Peterson, L. Grabow, T. Brennan, B. Shong, C. Ooi, D. Wu, C. Li, A. Kushwaha, A. Medford, F. Mbuga, L. Li, J. Nørskov, *Top. Catal.* **2012**, *55*, 1276 – 1282.
[8] a) E. Shustorovich, H. Sellers, *Surf. Sci. Rep.* **1998**, *31*, 1 – 119; b) J. Kleis, J. Greeley, N. A. Romero, V. A. Morozov, H. Falsig, A. H. Larsen, J. Lu, J. J. Mortensen, M. Dułak, K. S. Thygesen, J. K. Nørskov, K. W. Jacobsen, *Catal. Lett.* **2011**, *141*, 1067 – 1071.
[9] F. Calle-Vallejo, J. I. Martinez, J. M. Garcia-Lastra, J. Rossmeisl, M. T. M. Koper, *Phys. Rev. Lett.* **2012**, *108*, 116103.
[10] A. Eichler, J. Hafner, J. Furthmüller, G. Kresse, *Surf. Sci.* **1996**, *346*, 300 – 321.
[11] I. J. Robertson, M. C. Payne, V. Heine, *Europhys. Lett.* **1991**, *15*, 301 – 306.
[12] J. R. Kitchin, J. K. Nørskov, M. A. Barteau, J. G. Chen, *J. Chem. Phys.* **2004**, *120*, 10240 – 10246.
[13] T. Jiang, D. J. Mowbray, S. Dobrin, H. Falsig, B. Hvolbæk, T. Bligaard, J. K. Nørskov, *J. Phys. Chem. C* **2009**, *113*, 10548 – 10553.
[14] S. Kurth, J. P. Perdew, P. Blaha, *Int. J. Quantum Chem.* **1999**, *75*, 889 – 909.
[15] G. Kresse, J. Furthmüller, *Phys. Rev. B* **1996**, *54*, 11169 – 11186.

